We are IntechOpen, the world's leading publisher of Open Access books Built by scientists, for scientists

6,900
Open access books available

186,000
International authors and editors

200M
Downloads

154
Countries delivered to

Our authors are among the

TOP 1%
most cited scientists

12.2%
Contributors from top 500 universities

CLARIVATE ANALYTICS
BOOK CITATION INDEX
INDEXED

WEB OF SCIENCE™

Selection of our books indexed in the Book Citation Index
in Web of Science™ Core Collection (BKCI)

Interested in publishing with us?
Contact book.department@intechopen.com

Numbers displayed above are based on latest data collected.
For more information visit www.intechopen.com

3

Bending Deformation and Fatigue Properties of Precision-Casting TiNi Shape Memory Alloy Brain Spatula

Hisaaki Tobushi[1], Kazuhiro Kitamura[2],
Yukiharu Yoshimi[3] and Kousuke Date[1]
[1]Department of Mechanical Engineering, Aichi Institute of Technology
1247 Yachigusa, Yakusa-cho, Toyota, 470-0392, Japan
[2]Department of Technology Education, Aich University of Education,
Hirosawa 1, Igaya-cho, Kariya, 448-8542, Japan
[3]Yoshimi, Inc., 1-43 Kitasaki-cho, Obu, 474-0002, Japan
E-mail: tobushi@aitech.ac.jp

Abstract

In order to develop a brain spatula or a brain retractor made of a shape memory alloy (SMA), the bending characteristics of the brain spatula of TiNi SMA made by the precision casting were discussed based on the tensile deformation properties of the existing copper and the TiNi rolled-SMA. The fatigue properties of these materials were also investigated by the pulsating- and alternating-plane bending fatigue tests. The results obtained can be summarized as follows. (1) Based on the yield stress and the modulus of elasticity of the copper and the SMA, the bending deformation properties of an SMA-brain spatula were estimated by assuming the condition to use the brain spatula as the bending of a cantilever. With respect to the SMA-brain spatula for the same length and width as the existing copper-brain spatula, if the thickness of the new cast-SMA brain spatula is 1.2 times and that of the conventional rolled-SMA brain spatula is 1.3 times as large as that of the existing copper one, the SMA-brain spatula can hold the same bending rigidity and can be bent by almost the same force as the existing copper one. (2) With respect to the alternating- and pulsating-plane bending fatigue, the fatigue life of both the copper and the SMAs in the region of low-cycle fatigue is expressed by a power function of the maximum bending strain. The fatigue life of the conventional rolled SMA and the new cast SMA is longer than that of the existing copper. The fatigue life of the new cast and rolled SMAs in the pulsating-plane bending is longer than that in the alternating-plane bending. (3) The above mentioned characteristics of the SMA-brain spatula obtained in this study will be substantially applied to the development not only for the brain spatula but also for other retractors and instruments used in other surgery operations.

Keywords: Shape Memory Alloy, Brain Spatula, Titanium-Nickel Alloy, Fatigue, Precision Casting, Bending

1. Introduction

The shape memory effect (SME) and superelasticity (SE) appear in a shape memory alloy (SMA). The strain of several percents is recovered by heating for the SME and by unloading for the SE. These characteristics occur due to the martensitic transformation (MT) and its reverse transformation. Large recovery stress, energy dissipation and storage which appear owing to the MT can be used in the SMA [1-5]. The development of applications of the SMA as the intelligent materials has therefore attracted the worldwide attention. The SMA has been used in the wide fields of industry, electric products, medical devices, leisure and so on.

A brain spatula or a brain retractor is used as an instrument in a surgical operation of a brain. This instrument is used to hold the opened state of the brain during the operation of the cerebral tumor which is located in the inner part of the brain. An image of the brain spatula used in the operation is shown in figure 1. As shown in figure 1, the brain spatula is used in the bent form, fitting it to the shape and depth of each patient's brain. After the operation, the brain spatula is struck with a mallet to recover the original flat plane followed by the treatment in a sterilizer by heating and is used again thereafter. The main material used to the existing brain spatula is copper. Since the irrecoverable unevenness appears on the surface of the brain spatula after the use, it is disposed after using several times. If the SMA is used for the brain spatula, the brain spatula used in the bent form regains its original flat shape automatically based on the SME through the treatment of sterilization by heating in the autoclave. Therefore, since the SMA-brain spatula not only saves the time to strike with a mallet to regain the original flat shape but also recovers its original shape automatically, the appearance of the uneven plastic deformation is inhibited and the spatula can be used times out of number.

The TiNi SMA products made by the precision casting utilizing the lost-wax process from a self-combustion high-temperature synthesis method have been newly developed [6]. The brain spatula needs various shapes corresponding to the brain of each patient. TiNi SMA is very hard to form the complex shape of the products. An example of the TiNi SMA-brain spatula made by the precision casting is shown in figure 2. The TiNi SMA-brain spatula with complex shape can be easily produced by the precision casting.
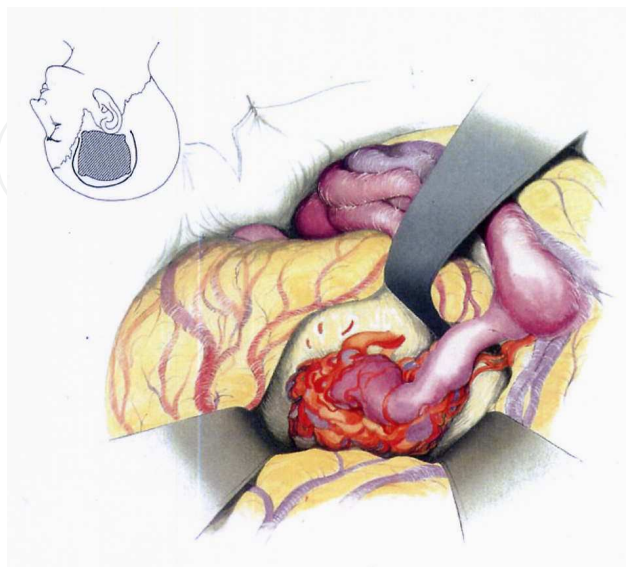

Fig. 1. Image of brain spatula in operation
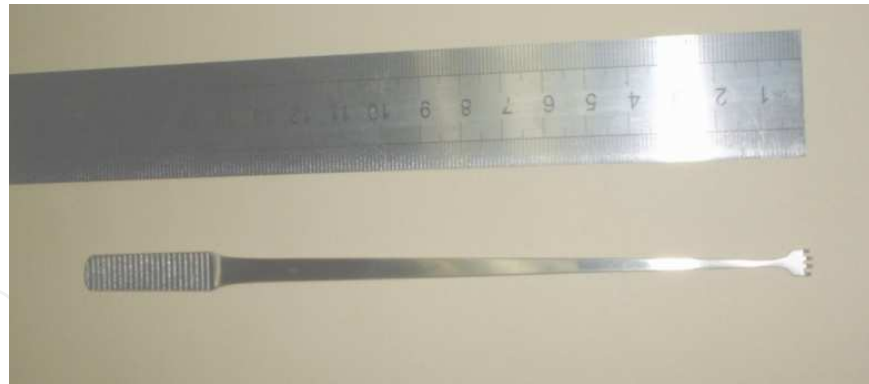
(a) Whole rake-type brain spatula

(b) Brain spatula just after
precision casting

(c) Tip of rake-type brain spatula

Fig. 2. Example of TiNi SMA-brain spatula made by the precision casting

The required conditions for the brain spatula are the fact that it can be bent in an arbitrary shape to fit it to the brain of a patient in the operation and it has enough rigidity to hold the opened state of the brain during the operation. These characteristics can be prescribed based on the bending deformation properties of the brain spatula including the bending rigidity. In order to evaluate the reliability of the brain spatula from the view point of safety, the fatigue properties of the materials are crucial. The brain spatula is subjected to cyclic plane bending. The plane-bending fatigue properties of TiNi SMA for the brain spatula have not been reported till now.

In the present study, in order to develop the SMA-brain spatula, the stress-strain relations of the new cast TiNi SMA, the conventional rolled TiNi SMA and the copper used for the existing brain spatula were examined by the tension tests. The shape and dimension which are required for the SMA-brain spatula were investigated based on the bending deformation properties of the strip cantilever. The fatigue properties of the materials which are very important in the practical cyclic use were also investigated.

2. Experimental Method

2.1 Materials and specimens

The materials used in the experiment were the new cast Ti-49.7at%Ni SMA, the conventional rolled Ti-50.0at%Ni SMA, and the existing copper brain spatula. The new cast SMA was made by the precision casting utilizing the lost-wax process from a self-combustion high-temperature synthesis method [6]. A flat plane of the rolled and the cast SMA was shape-memorized by fixing in a flat plane for 40 min at 753 K in the furnace followed by quenching in water. The starting and finishing temperatures of the MT M_s and M_f and those of the reverse transformation A_s and A_f of the SMAs were obtained from the DSC (differential scanning calorimetric) test. The values obtained were M_s = 326 K, M_f = 312 K, A_s = 342 K, A_f = 365 K for the rolled SMA and M_s = 358 K, M_f = 283 K, A_s = 314 K, A_f = 386 K for the cast SMA. The specimens used in the tension test were the uniform rectangular bars with a thickness of t = 1.0 mm, a width of w = 1.2 mm and a length of l = 160 mm for the rolled and cast SMAs, and t = 1.0 mm, w = 8.5 mm and l=140 mm for the copper. In the fatigue test, all specimens were the bars with t = 1.0 mm, w=1.2 mm and l = 80 mm.

2.2 Experimental apparatus

An SMA characteristic testing machine was used for the tension test [7]. The testing machine was composed of a tension machine for loading and unloading and a heating–cooling device to control temperature. Displacement of the specimen was measured by an extensometer with a gauge length of 50 mm.

① Specimen   ⑥ Power source
② Grip   ⑦ Crank 1
③ Speed controller ⑧ Crank 2
④ Counter   ⑨ Bearing
⑤ Motor
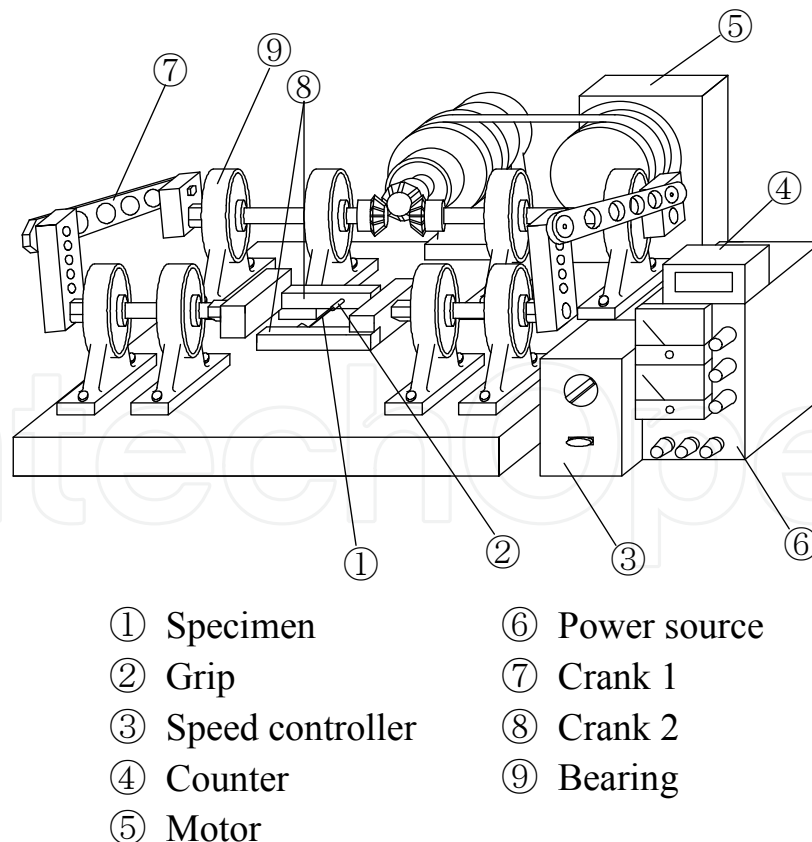
Fig. 3. Experimental apparatus for alternating-plane bending fatigue test

An alternating-plane bending fatigue testing machine [8] used in the fatigue test is shown in figure 3. In the fatigue testing machine, the maximum bending strain occurs at the central part of the specimen □, and the tensile and compressive bending strains occur alternately. A pulsating-plane bending fatigue testing machine [9] was also used in the fatigue test. In the alternating- and pulsating-plane bending tests, the maximum bending strain on the surface of the specimen was selected and the number of cycles to failure was obtained under a constant frequency. A scanning electron microscope (SEM) was used to observe the fracture surface of specimen.

2.3 Experimental procedure

The tension tests were carried out under a constant strain rate in air at room temperature below the M_f point of the SMA bars. Since the yielding of the SMA occurs under low stress in the case of the M-phase, the SMA-brain spatula can be easily bent by small force. For the M-phase SMA bar, the residual strain appears after unloading. The SMA bars with the residual strain were heated up to temperatures above the A_f point under no load. In the heating process of the SMA bars, the residual strain diminishes due to the reverse transformation between the A_s and A_f points.

The alternating- and pulsating-plane bending fatigue tests were carried out in air at room temperature. Every specimen was fractured in the central part of its length between grips where the bending strain takes the maximum value. The maximum bending strain ε_m on the surface of the specimen was obtained from the radius of curvature at the point of fracture. The frequency f was 8.33 Hz (500 cpm) and 3.33 Hz (200 cpm).

3. Deformation properties of materials used for brain spatula

3.1 Tensile deformation properties

The stress-strain curves of the copper, the rolled and the cast SMAs obtained from the tension test under a strain rate of $d\varepsilon/dt = 2 \times 10^{-4}$ s^{-1} are shown in figure 4. As can be seen in figure 4, the linear elastic deformation occurs in the initial loading stage and the yielding occurs thereafter. The modulus of elasticity E determined from a slope of the initial stress-strain curves is $E = 40$ GPa for the rolled SMA, $E = 54$ GPa for the cast SMA and $E = 95$ GPa for the copper. Approximating the elastic and yield regions of the stress-strain curves by two straight lines, the yield stress σ_y was determined from an intersection of two lines. The yield stress was $\sigma_y = 68$ MPa for the rolled SMA, $\sigma_y = 168$ MPa for the cast SMA and $\sigma_y = 240$ MPa for the copper. In the case of the copper, the deformation above a strain of 0.2 % occurs due to the plastic deformation with dislocations. Therefore, in the unloading process from a strain of 4 %, strain is recovered by 0.25 % due to the elastic deformation and the residual strain appears as the permanent strain. In the case of the SMAs, since the material is in the M-phase at room temperature below the M_f point, the yielding occurs due to the rearrangement of the M-phase. In the unloading process from a strain of 4 %, strain is recovered by 0.6 % and 0.8 % for the rolled and the cast SMAs, respectively, and the residual strain of 3.4 % and 3.2 % appears after unloading.
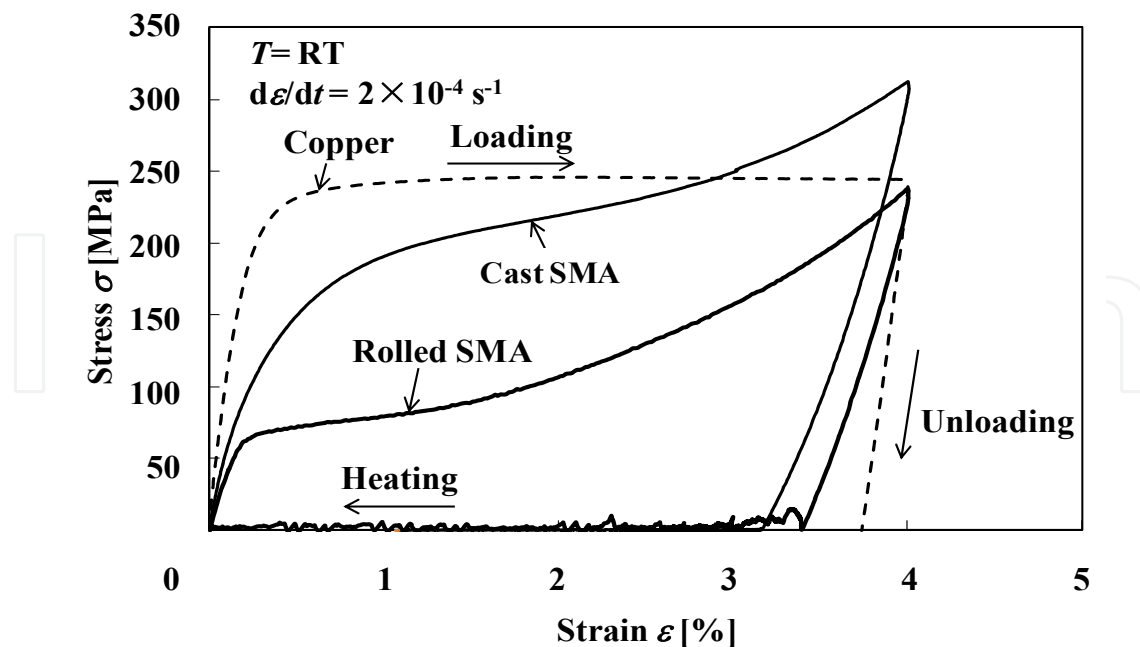
Fig. 4. Stress-strain curves of copper, rolled SMA and cast SMA used for brain spatula in tension

The relationship between strain and temperature of the cast and rolled SMAs obtained from the tension test with unloading followed by heating under no load is shown in figure 5. The symbols $A_{s:C}$, $A_{s:R}$, $A_{f:C}$ and $A_{f:R}$ shown in figure 5 represent the reverse-transformation starting and finishing temperatures of the cast and rolled SMAs, respectively. In the heating process under no load, strain starts to be recovered gradually around A_s and disappears perfectly around A_f. The SME to show this strain recovery occurs due to the reverse transformation from the M-phase to the parent (austenite) phase.

3.2 Comparison of characteristic values for deformation

The values of the modulus of elasticity E, the yield stress σ_y and the yield strain ε_y of the copper, the rolled and the cast SMAs obtained from the tension test are shown in table 1. As can be seen from table 1, both the modulus of elasticity and the yield stress of the rolled and the cast SMAs are lower than those of the copper. These differences affect the deformation residence to bend the brain spatula and the bending rigidity to hold the opened shape of the brain during the operation. In the next section, the bending deformation properties of the brain spatulas made of these materials will be discussed.
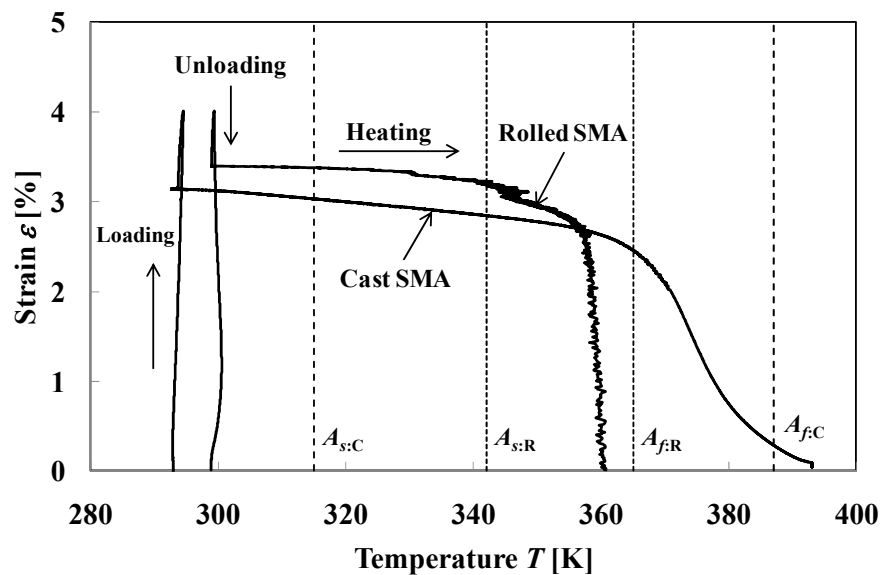
Fig. 5. Strain-temperature curves of rolled SMA and cast SMA in tension with unloading followed by heating under no-load

Table 1. Values of modulus of elasticity, yield stress and yield strain for copper, rolled SMA and cast SMA

	Copper	Rolled SMA (M-phase)	Cast SMA (M-phase)
Modulus of elasticity E [GPa]	95	40	54
Yield stress σ_y [MPa]	240	68	168
Yield strain ε_y [%]	0.25	0.17	0.34

4. Bending characteristics of copper- and SMA-brain spatulas

4.1 Elastic bending property of brain spatula

In order to design the SMA-brain spatula, it is important to evaluate the force which is necessary for a medical doctor to bend the brain spatula and the bending rigidity which is required to hold the opened shape of the brain during the operation. Discussing these bending deformation properties of the copper- and the SMA-brain spatulas, the characteristics required for the SMA-brain spatula will be clarified. Let us treat the bending of the existing brain spatula as the bending of a cantilever made of the strip with a uniform rectangular cross-section. The length of the strip is expressed by l, the width of the cross-section by w and the thickness by t. In order to hold the displacement of the opened part of the brain during the operation, it is required for the brain spatula to keep the bent form (see figure 1). This requirement can be evaluated by the maximum deflection of the cantilever

made of these materials. Let us consider the condition to obtain the same maximum deflection y_{max} by the same force F applied at the top of the cantilever. The maximum deflection of the cantilever y_{max} can be expressed by using the second moment of area I_z $= wt^3/12$ from the theory of elasticity as follows

$$y_{\max} = \frac{Fl^3}{3EI_z} = \frac{4Fl^3}{Ewt^3} \tag{1}$$

If the maximum deflection y_{max} expressed by Eq. (1) for the copper and the SMA strips subjected to the same force F coincides, the following equation is obtained

$$y_{\max} = \frac{4Fl_{Cu}^3}{E_{Cu} \cdot w_{Cu} \cdot t_{Cu}^3} = \frac{4Fl_{SMA}^3}{E_{SMA} \cdot w_{SMA} \cdot t_{SMA}^3} \tag{2}$$

From the view point of the practical operation of the brain, the width w and the length l of the SMA-brain spatula are expected to take the same values as those of the existing copper-brain spatula. Therefore, let us consider the condition that the length l and the width w of both spatulas coincide and only the thickness t differs. The thickness of SMA t_{SMA} becomes from Eq. (2) as follows

$$t_{SMA} = \sqrt[3]{\frac{E_{Cu}}{E_{SMA}}} t_{Cu} \tag{3}$$

The values of the modulus of elasticity E of the copper and the SMAs shown in table 1 are substituted in Eq. (3). As a result, if the thickness of the rolled-SMA spatula is 1.3 times and that of the cast-SMA spatula is 1.2 times as large as that of the copper one, the bending rigidity of both copper and SMA spatulas coincides and the same deflection can be obtained by the SMA-brain spatulas.

4.2 Plastic deformation resistance for bending

In the operation of the brain, a medical doctor bends the brain spatula to fit it to the shape and depth of the opened part of each patient's brain. The force to bend the brain spatula is valuated by the force applied at the top of the cantilever to obtain the required maximum bending strain. The yield region appears in the surface element of the cantilever during bending. The elastic and yield regions of the strip in bending are shown in figure 6. The schematic distributions of the bending strain and stress in the strip are shown in figures 7 and 8, respectively. In these figures, the maximum bending strain, the yield strain and the yield stress are denoted by ε_m, ε_y and σ_y, respectively. It is assumed that the yield stress σ_y in tension is the same as that in compression and is constant in the yield region.

Yield region in tension

Elastic region

M

x

M

Yield region in compression
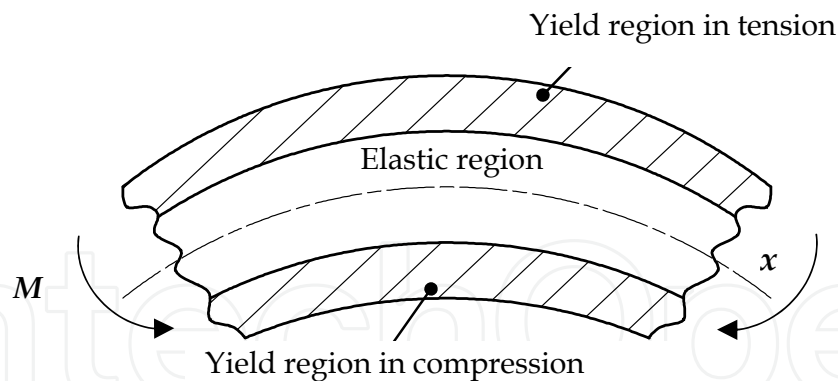
Fig. 6. Elastic and yield regions of strip in bending
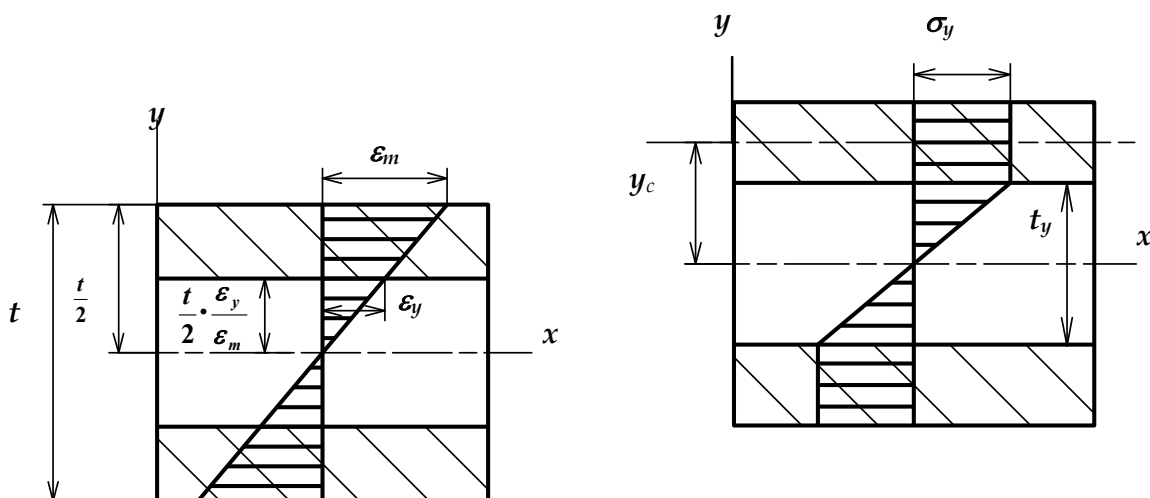
Fig. 7. Bending strain distribution in the strip   Fig. 8. Bending stress distribution in the strip

At first, let us consider the bending moment M_e which is required to obtain the elastic region of the strip in bending. The thickness of the elastic region t_y is $t_y = (\varepsilon_y/\varepsilon_m)t$. Since the maximum bending stress in the elastic region σ_{max} is the same as the yield stress σ_y, the bending moment required for the elastic region M_e is $M_e = \sigma_y \cdot Z$, where Z denotes the section modulus and $Z = wt_y^2/6$. Therefore, the bending moment M_e for the elastic region is

$$M_e = \frac{\sigma_y wt^2}{6}\left(\frac{\varepsilon_y}{\varepsilon_m}\right)^2 \tag{4}$$

Next, let us consider the bending moment M_y required to cause the yield region of the strip. The center of the yield region y_c from the neutral axis z is

$$y_c = \frac{t}{4}\left(1 + \frac{\varepsilon_y}{\varepsilon_m}\right) \tag{5}$$

The area A of the yield region in the tension side on the cross section is

$$A = \frac{wt}{2}\left(1 - \frac{\varepsilon_y}{\varepsilon_m}\right) \tag{6}$$

Considering the constant stress σ_y in the yield region and the symmetric condition in the tension and compression sides, the bending moment M_y required to cause the yield region is obtained as follows.

$$M_y = \sigma_y \cdot A \cdot 2y_c = \frac{\sigma_y wt^2}{4}\left\{1 - \left(\frac{\varepsilon_y}{\varepsilon_m}\right)^2\right\} \tag{7}$$

The total bending moment M required to bend the brain spatula is given by a sum of the bending moment M_e for the elastic region and the bending moment M_y for the yield region.

$$M = M_e + M_y = \frac{\sigma_y wt^2}{12}\left\{3 - \left(\frac{\varepsilon_y}{\varepsilon_m}\right)^2\right\} \tag{8}$$

Since the bending moment M is $\boldsymbol{M = Fl}$, the force required is

$$F = \frac{\sigma_y wt^2}{12l}\left\{3 - \left(\frac{\varepsilon_y}{\varepsilon_m}\right)^2\right\} \tag{9}$$

The condition, that the forces required to bend the copper-brain spatula and the SMA-brain spatula coincide, is as follows.

$$F = \frac{\sigma_{yCu} w_{Cu} t_{Cu}^2}{12l_{Cu}}\left\{3 - \left(\frac{\varepsilon_{yCu}}{\varepsilon_{mCu}}\right)^2\right\} = \frac{\sigma_{ySMA} w_{SMA} t_{SMA}^2}{12l_{SMA}}\left\{3 - \left(\frac{\varepsilon_{ySMA}}{\varepsilon_{mSMA}}\right)^2\right\} \tag{10}$$

If the length l, the width w and the maximum bending strain ε_m of both spatulas coincide and only the thickness differs, the thickness of the SMA-brain spatula is

$$t_{SMA} = t_{Cu} \left[\frac{\sigma_{yCu} \left\{ 3 - \left(\frac{\varepsilon_{yCu}}{\varepsilon_m} \right)^2 \right\}}{\sigma_{ySMA} \left\{ 3 - \left(\frac{\varepsilon_{ySMA}}{\varepsilon_m} \right)^2 \right\}} \right]^{\frac{1}{2}} \qquad (11)$$

The yield stress σ_y and the yield strain ε_y of each material are shown in table 1. Using these values, the thickness of the SMA-brain spatula t_{SMA} was obtained from Eq. (11). The calculated results of t_{SMA} compared with the thickness of the copper-brain spatula t_{Cu} for the maximum bending strain ε_m = 1- 4 % are shown in table 2. If the thickness shown in table 2 is used, the SMA-brain spatula can be bent by the same force as that required for the existing copper-brain spatula. As can be seen from table 2, the maximum bending strain ε_m affects slightly on the ratio of t_{SMA} to t_{Cu}. If the thicknesses of the rolled- and the cast-SMA brain spatula are 1.88 times and 1.16 times as large as that of the copper-brain spatula, respectively, the SMA-brain spatula can be bent by the same force as the existing copper-brain spatula.

4.3 Shape of SMA-brain spatula

Based on the discussion in the sections 4.1 and 4.2, it has been clarified that, if the length and the width of the rolled-SMA brain spatula are the same as those of the existing copper-brain spatula and the thickness of the rolled-SMA brain spatula is 1.3 times as large as that of the copper one, the rolled-SMA brain spatula can hold the same bending rigidity and can be bent easily by the smaller force than the copper one. If the thickness of the cast-SMA brain spatula is 1.2 times as large as that of the copper one, the cast-SMA brain spatula can hold the same bending rigidity and can be bent by almost the same force as the existing copper one.

Table 2. Thickness of SMA-brain spatula compared with that of copper-brain spatula t_{Cu} required to bend both spatulas by the same force for various maximum bending strains

Maximum bending strain	Thickness of Rolled SMA	Thickness of Cast SMA
ε_m = 1 %	1.87 t_{Cu}	1.17 t_{Cu}
ε_m = 2 %	1.88 t_{Cu}	1.16 t_{Cu}
ε_m = 3 %	1.88 t_{Cu}	1.16 t_{Cu}
ε_m = 4 %	1.88 t_{Cu}	1.16 t_{Cu}

5. Bending fatigue properties

5.1 Fatigue life in alternating-plane bending

The relationships between the maximum bending strain ε_m and the number of cycles to failure N_f obtained from the alternating-plane bending fatigue test for the rolled SMA, the cast SMA and the copper are shown in figure 9.
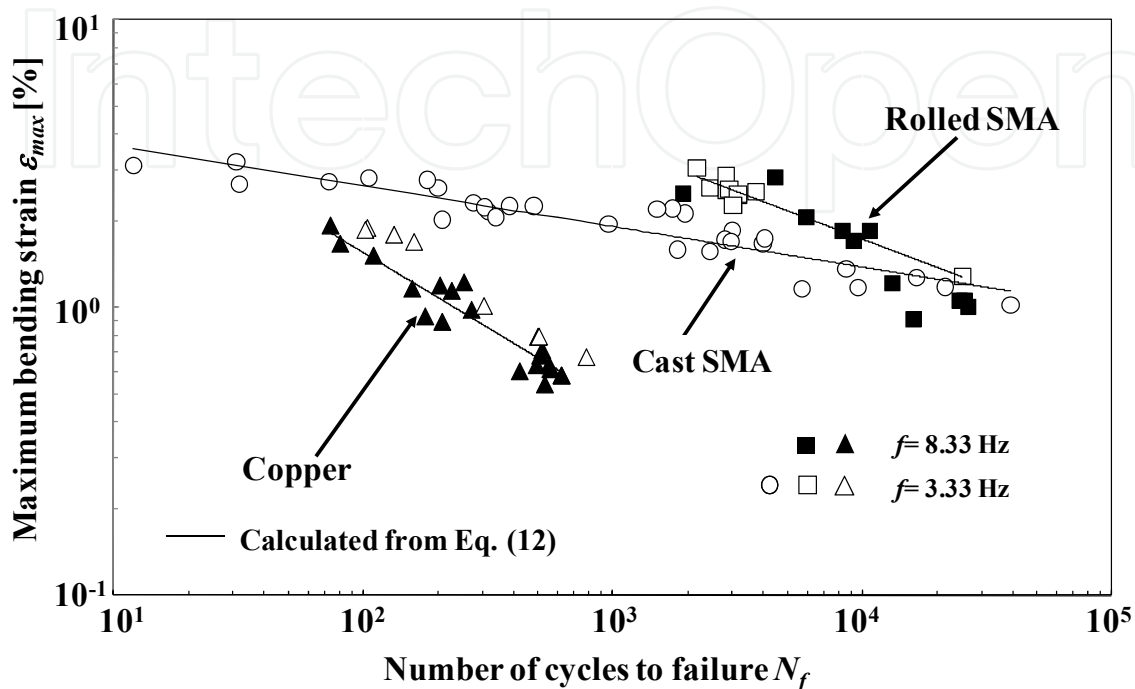

Fig. 9. Fatigue life curves of copper, rolled SMA and cast SMA used for brain spatula in alternating-plane bending

In figure 9, the larger the ε_m, the smaller the N_f for all materials. The fatigue life of the rolled SMA is longer than that of the copper by 100 times. The fatigue life of the cast SMA is longer that of the copper by 100 times in the region of small ε_m and by 10 times in the region of large ε_m. The fatigue life of the copper is several hundred cycles at $\varepsilon_m = 1$ %. This fatigue life is almost the same as that in the low-cycle fatigue of normal metals [10]. In the case of the copper, the yield strain is caused by the slip of crystals and the plastic deformation occurs repeatedly, resulting in the short fatigue life. In the case of the SMAs, the yield strain is caused not by the permanent slip but by the recoverable rearrangement of the M-phase, resulting in the long fatigue life. In the case of the cast SMA, as observed in figure 4, stress increases with an increase in strain, resulting in the shorter fatigue life with an increase in the maximum bending strain. The influence of the frequency on the fatigue life for all materials is not clear for f =3.33 Hz and 8.33 Hz. In the case of a TiNi SMA wire, the lower the frequency, the longer the fatigue life is [11]. The frequency of the SMA-brain spatula in the practical use should be lower than f =3.33 Hz and 8.33 Hz. Therefore, the fatigue life in the practical use will be longer than that obtained in the present study.

In figure 9, the fatigue life curves of all materials in the low-cycle fatigue region can be approximated by the straight lines. Since the relationships between ε_m and N_f can be expressed

by the straight lines on the logarithmic graph, the relationship can be expressed by a power function similar to the fatigue life for the TiNi SMA wires and tubes [12] as follows

$$\varepsilon_m \cdot N_f{}^\beta = \alpha$$

$\beta = 0.58$, $\alpha = 25\%$: Copper
$\beta = 0.41$, $\alpha = 67\%$: Rolled SMA   (12)
$\beta = 0.14$, $\alpha = 5\%$: Cast SMA

where α and β denote ε_m in $N_f = 1$ and the slope of the log ε_m – log N_f curves, respectively. The calculated results by Eq. (12) are shown by the solid lines in figure 9. As can be seen, the overall inclinations are well approximated by the solid lines.

5.2 Fatigue life in pulsating-plane bending

The relationships between the maximum bending strain ε_m and the number of cycles to failure N_f obtained from the pulsating-plane bending fatigue test for the cast SMA, the rolled SMA and the copper are shown in figure 10.

In figure 10, the larger the ε_m, the smaller the N_f for all materials. The fatigue life of the rolled SMA is longer than that of the copper by 100 times. The fatigue life of the cast SMA is longer that of the copper by 40 times. The fatigue life of the copper is two thousands cycles at $\varepsilon_m = 2$ %. In the case of the cast SMA, as observed in figure 4, the yield stress is higher than that of the rolled SMA, resulting in the shorter fatigue life than the rolled SMA.

In figure 10, the fatigue life curves of all materials in the low-cycle fatigue region can be approximated by the straight lines. The relationship can be expressed by a power function similar to Eq. (12) as follows

$$\varepsilon_m \cdot N_f{}^\beta = \alpha$$

$\beta = 0.35$, $\alpha = 26\%$: Copper
$\beta = 0.29$, $\alpha = 49\%$: Cast SMA   (13)
$\beta = 0.26$, $\alpha = 43\%$: Rolled SMA

The calculated results by Eq. (13) are shown by the solid lines in figure 10. As can be seen, the overall inclinations are well approximated by the solid lines.
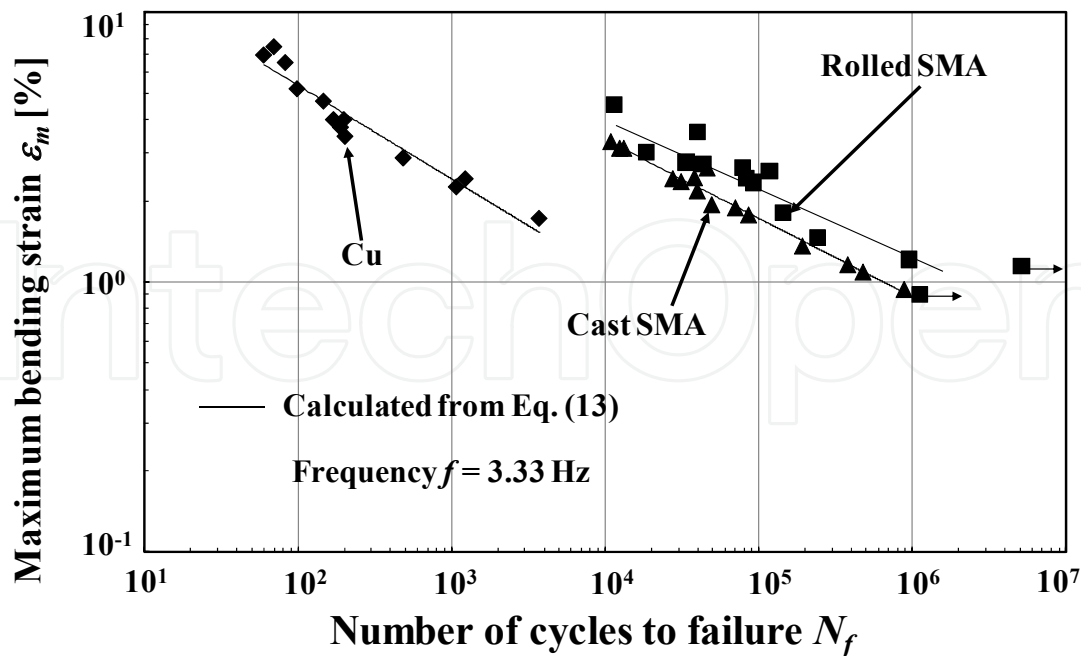
Fig. 10. Fatigue-life curves of copper, rolled SMA and cast SMA used for brain spatula in pulsating-plane bending

5.3 Comparison of fatigue life

The relationships between the maximum bending strain ε_m and the number of cycles to failure N_f obtained from the alternating- and pulsating-plane bending fatigue tests for the rolled and cast SMAs are shown in figures 11 and 12, respectively. In figures 11 and 12, the fatigue life in alternating-plane bending is shorter than that in the pulsating-plane bending. The dissipated work in each cycle of the alternating-plane bending is larger than that in the pulsating-plane bending. The fatigue damage is greater in the alternating-plane bending, and therefore the fatigue life in the alternating-plane bending is shorter than that in the pulsating-plane bending. The influence of the dissipated work W_d on the fatigue life between the alternating- and pulsating-plane bendings can be explained as follows. The stress-strain diagram and the dissipated work W_d at each cycle in the pulsating- and alternating-plane bendings are schematically shown in figure13. In figure 13, it is assumed that the yield stress σ_M is constant in the stress-plateau region and takes the same value in tension and compression. The area surrounded by the hysteresis loop denotes the dissipated work W_d per unit volume in each cycle. The dissipated work W_d is expressed by the following equation in the pulsating-plane bending

$$W_d = 2\sigma_M \left(\varepsilon_m - \frac{2\sigma_M}{E} \right) \tag{14}$$

and that in alternating-plane bending

$$W_d = 2\sigma_M \left(2\varepsilon_m - \frac{2\sigma_M}{E} \right) \tag{15}$$

where E represents the elastic modulus. It can be seen from Eqs. (14) and (15) that W_d increases in proportion to both σ_M and ε_m. The values of the dissipated W_d for $\varepsilon_m=3\%$ by using Eqs. (14) and (15) are shown in Table 3. As can be seen in Table 3, the value of W_d for the cast SMA in the case of the alternating-plane bending is very large compared to that of the pulsating-plane bending. Therefore, in the case of the cast SMA, the fatigue life of the alternating-plane bending is short for large maximum bending strain ε_m.
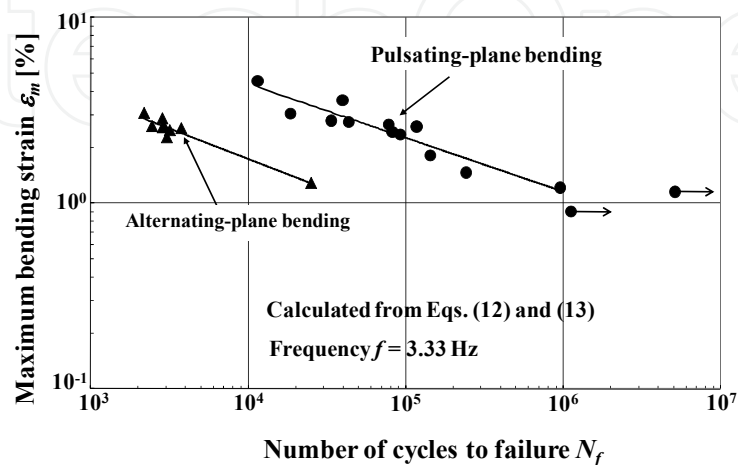
Fig. 11. Relationship between maximum bending strain and number of cycles to failure of rolled SMA in pulsating-plane and alternating-plane bending
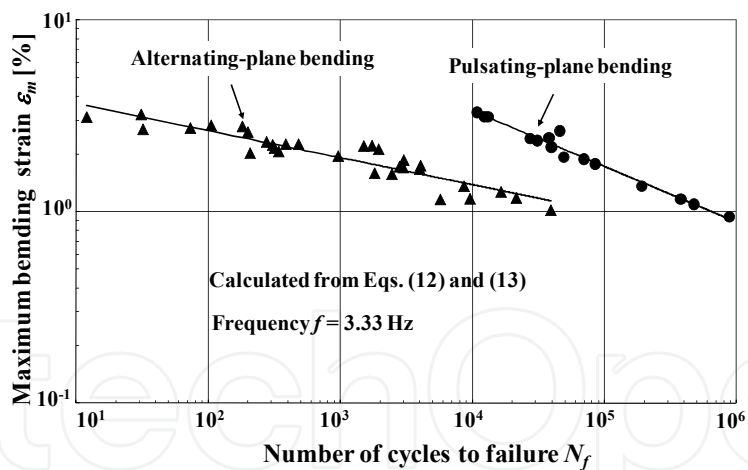
Fig. 12. Fatigue-life curves of cast SMA used for brain spatula in pulsating-plane and alternating-plane bending

(a) Pulsating–plane bending   (b) Alternating–plane bending
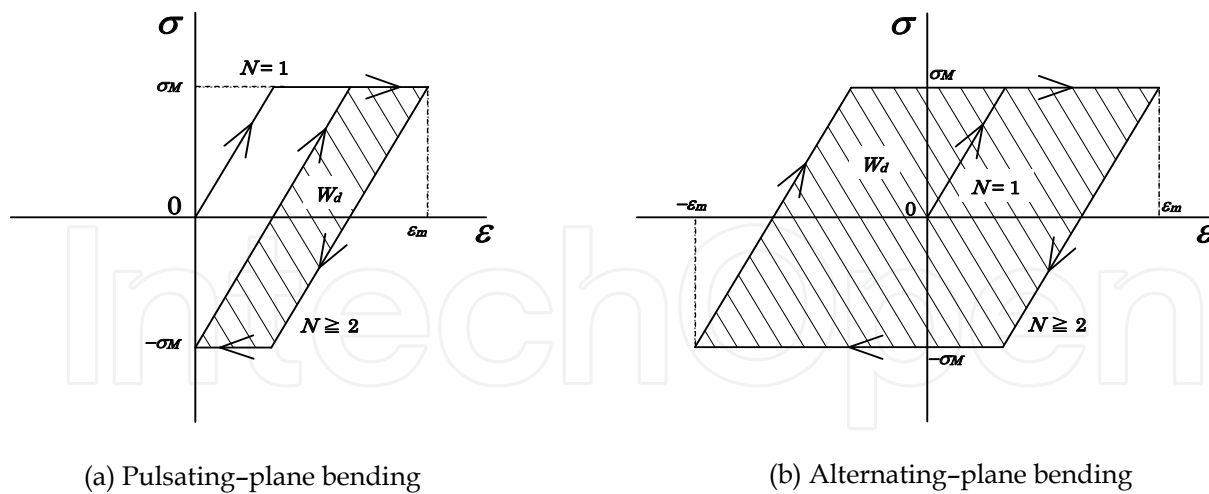
Fig. 13. Stress-strain diagram and dissipated work W_d at each cycle in pulsating–plane bending and alternating-plane bending

Table 3. Values of dissipated work W_d in pulsating- and alternating-plane bendings for e_m = 3%

Materials	Dissipated work W_d (MJ/m³)	
	Pulsating bending	Alternating bending
Rolled SMA	3.6	7.7
Cast SMA	8.0	18
Copper	12	26

5.4 Temperature rise under cyclic bending

The surface element of the specimen is subjected to the dissipated work in each cycle as discussed in section 5.3. Therefore, temperature of the specimen increases during cyclic bending. The temperature on the surface of the central part of the rolled SMA was measured by using a thermocouple in the case of the alternating-plane bending at a frequency of f =3.33 Hz. The relationship between the temperature rise ΔT and time is shown in figure 14. The temperature increases rapidly in the early 20 s. After 20 s, the amount of generated heat and released heat matches each other and ΔT saturates at a certain value.

The relationship between the saturated temperature rise ΔT_s and the maximum bending strain ε_m for the rolled and cast SMAs at f = 3.33Hz is shown in figure 15. The saturated temperature rise ΔT_s increases in proportion to the maximum bending strain ε_m. The value of ΔT_s for the cast SMA is a little larger than that for the rolled SMA, and is about 30K at ε_m =3%. The yield stress σ_M increases in proportion to temperature rise ΔT by 5MPa/K for TiNi SMA. Therefore, if ΔT = 30K, the yield stress increases by 150MPa. This means the fact that the fatigue damage is large in the case of alternating-plane bending for the large ε_m. In the case of practical use of the brain spatula, the frequency is low and the temperature rise is small, resulting in the longer fatigue life than that obtained in the present study.
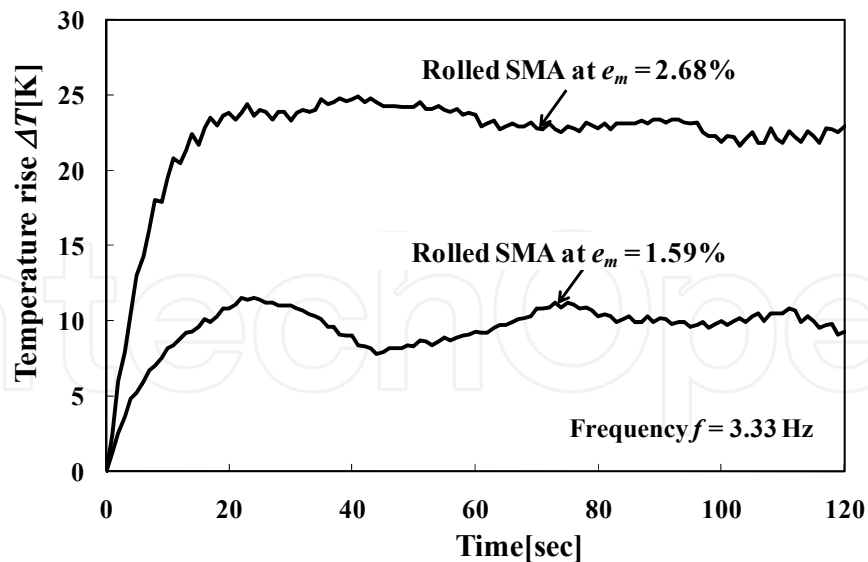
Fig. 14. Relationships between temperature rise and time for rolled SMA in alternating-plane bending at f =3.33 Hz
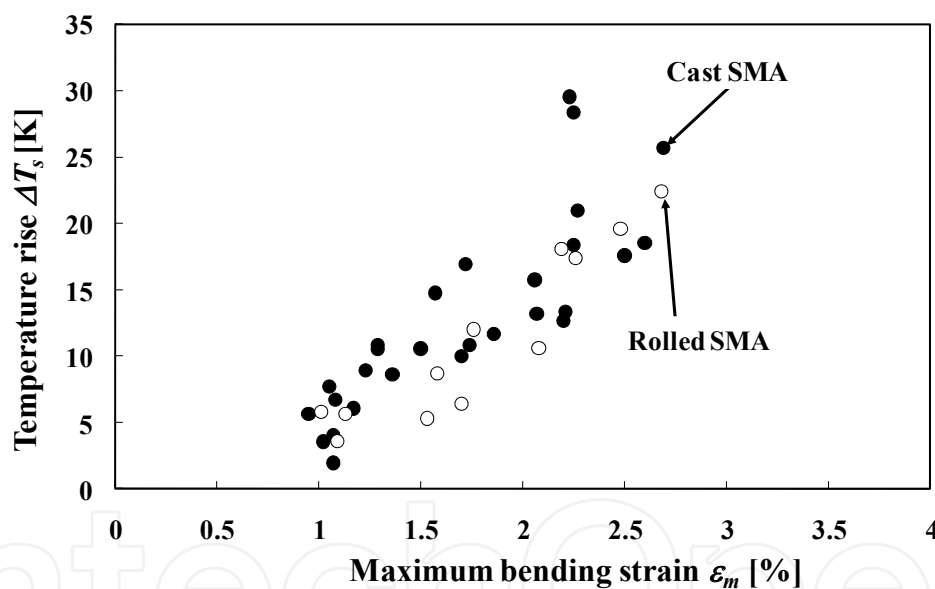
Fig. 15. Relationships between saturated temperature rise and maximum bending strain in alternating-plane bending at f =3.33 Hz

5.5 Observation of Fracture Surface.

The SEM photograph of the fracture surface for the rolled SMA in the case of the pulsating-plane bending at ε_m = 2.66% and N_f = 78081 cycles is shown in figure 16. As can be seen, the fatigue crack nucleates at one corner and grows into the central part. The crack growth rate is higher along the surface since the stress of the surface element is higher than that of the central element. This fatigue crack growth is the same inclination as that observed in the case of the alternating-plane bending for the rolled SMA.

The SEM photograph of the fracture surface for the cast SMA in the case of the pulsating-plane bending fatigue at ε_m = 2.41% and N_f = 27417 cycles is shown in figure 17. The fatigue crack nucleates at one corner and grows into the central part. The overall inclination of the fatigue crack growth is similar to that for the rolled SMA shown in figure 16.

The SEM photograph of the fracture surface for the cast SMA in the case of the alternating-plane bending fatigue at ε_m = 1.74% and N_f = 4052 cycles is shown in figure 18. The casting defect is observed in the neighbourhood of the surface and the fatigue crack grows from this casting defect. If the casting defect exists on the surface element, the fatigue crack starts in the early cycle. Therefore the development of casting method without defects is the future subject.
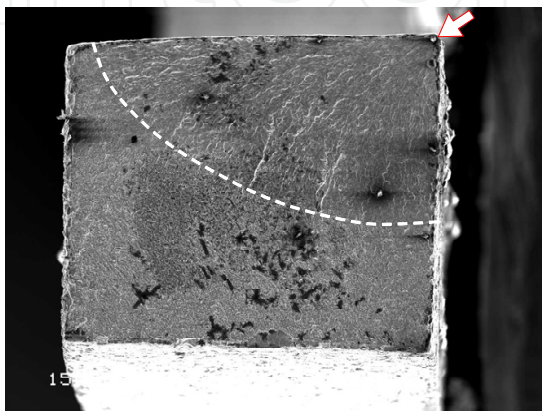
Fig. 16. SEM photograph of fracture surface for rolled SMA in pulsating-plane bending fatigue
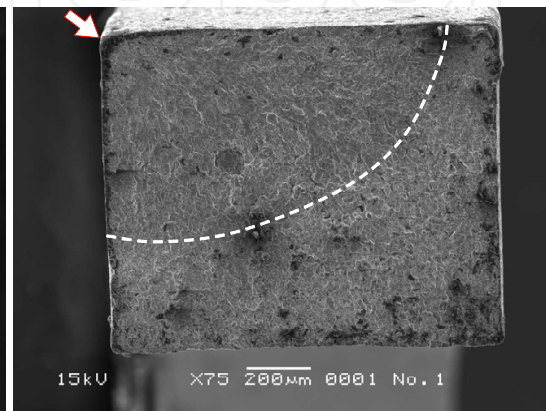
Fig. 17. SEM photograph of fracture surface for cast SMA in pulsating-plane bending fatigue
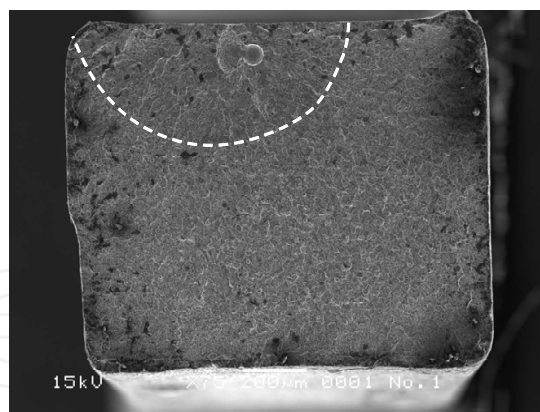
Fig. 18. SEM photograph of fracture surface for cast SMA in alternating-plane bending fatigue

6. Conclusions

In order to develop the SMA-brain spatula, the mechanical characteristics of the TiNi cast- and rolled-SMAs and the copper used for the brain spatula were compared based on the tensile deformation properties, and the characteristics of the SMA-brain spatula were discussed. The fatigue properties of these materials were also investigated by the pulsating-

and alternating-plane bending fatigue tests. The results obtained can be summarized as follows.

Based on the yield stress and the modulus of elasticity of the copper and the TiNi SMAs, the bending deformation properties of the SMA-brain spatula were estimated by assuming the condition to use the brain spatula as the bending of the strip cantilever. With respect to the SMA-brain spatula for the same length and width as the existing copper one, if the thickness of the conventional rolled-SMA spatula is 1.3 times as large as that of the existing copper-brain spatula, the SMA spatula can hold the same bending rigidity and can be bent by smaller force than the existing copper one. If the thickness of the new cast-SMA spatula is 1.2 times as large as that of the existing-copper spatula, the SMA spatula can hold the same bending rigidity and can be bent by almost the same force as the existing copper one.

With respect to the alternating- and pulsating-plane bending fatigue, the fatigue life of both the copper and the SMAs in the region of low-cycle fatigue is expressed by a power function of the maximum bending strain. The fatigue life of the conventional rolled SMA and the new cast SMA is longer than that of the existing copper. The fatigue life of the new cast and rolled SMAs in the pulsating-plane bending is longer than that in the alternating-plane bending.

The above mentioned characteristics of the SMA-brain spatula obtained in this study will be substantially applied to the development not only for the brain spatula but also for other retractors and instruments used in other surgery operations.

Acknowledgment

7. References

[1] Funakubo H, ed. 1987, *Shape memory alloys*, Gordon and Breach Science Pub., 1-60

[2] Duerig T W, Melton K N, Stockel, D and Wayman C M eds., 1990, *Engineering Aspects of Shape Memory Alloys*, Butterworth-Heinemann, 1-35

[3] Saburi, T, ed. 2000, *Shape Memory Materials*, Trans Tech Pub., Switzerland.,

[4] Chu, Y. Y. and Zhao, L. C., eds., 2002, *Shape Memory Materials and Its Applications*, Trans Tech Pub., Switzerland.

[5] Otsuka, K. and Wayman, C. M., eds., 1998, *Shape Memory Materials*, Cambridge University Press, Cambridge.

[6] Yoshimi Y, Kitamura K, Tokuda M, Inaba T, Asai J and Watanabe Y, 2008, *Ti-Ni Shape Memory Alloys Precision Casting Products and Its Process*, Proc. Int. Conf. Shape Memory and Superelastic Tech., 387-396.

[7] Tobushi H, Tanaka K, Kimura K, Hori T and Sawada T, 1992, *JSME Inter. J.,* 35-3 278-284.

[8] Furuichi Y, Tobushi H, Ikawa T and Matsui R, 2003, *J. Materials: Design and Applications* 217-Part L 93-99.

[9] Tobushi, H., Okumura, K., Nakagawa, K. and Takata, K., Fatigue Properties of TiNi Shape Memory Alloy, Trans. Mater. Res. Soc. Jap., 26-1, 2001, pp. 347-350.

[10] Shigley J. E. and. Mischke C. R., 1989, *Mechanical Engineering Design, 5th ed.*, McGraw-Hill, New York, 270-274.

[11] Tobushi H, Nakahara T, Shimeno Y and Hashimoto T, 2000, *Low-Cycle Fatigue of TiNi Shape Memory Alloy and Formulation of Fatigue Life*, Trans. ASME, J. Eng. Mater. Tech., 122 186-191

[12] Matsui, R., Tobushi, H., Furuichi, Y. and Horikawa, H., Tensile Deformation and Rotating-Bending Fatigue Properties of a Highelastic Thin Wire, a Superelastic Thin Wire, and a Superelastic Thin Tube of NiTi Alloys, Trans. ASME, J. Eng. Mater. Tech., 126, (2004), pp. 384-391.
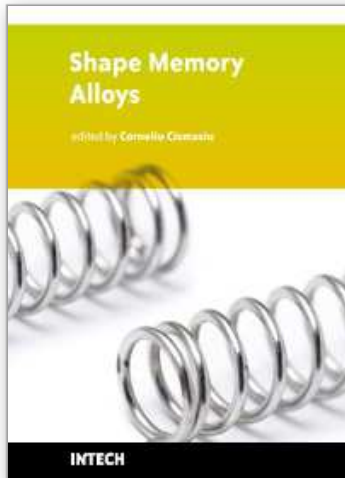
Shape Memory Alloys

Edited by Corneliu Cismasiu

In the last decades, the Shape Memory Alloys, with their peculiar thermo-mechanical properties, high corrosion and extraordinary fatigue resistance, have become more popular in research and engineering applications. This book contains a number of relevant international contributions related to their properties, constitutive models and numerical simulation, medical and civil engineering applications, as well as aspects related to their processing.

How to reference

In order to correctly reference this scholarly work, feel free to copy and paste the following:

Hisaaki Tobushi, Kazuhiro Kitamura, Yukiharu Yoshimi and Kousuke Date (2010). Bending Deformation and Fatigue Properties of Precision-Casted TiNi Shape-Memory Alloy Brain Spatula, Shape Memory Alloys, Corneliu Cismasiu (Ed.), ISBN: 978-953-307-106-0, InTech, Available from: http://www.intechopen.com/books/shape-memory-alloys/bending-deformation-and-fatigue-properties-of-precision-casted-tini-shape-memory-alloy-brain-spatula

INTECH
open science | open minds